



## Unique Aluminum Effect of $\text{LiAl}_x\text{Mn}_{2-x}\text{O}_4$ Material in the 3 V Region

Yun-Sung Lee and Masaki Yoshio<sup>\*,z</sup>

Department of Applied Chemistry, Saga University, Saga 840-8502, Japan

$\text{LiMn}_2\text{O}_4$  and  $\text{LiAl}_{0.1}\text{Mn}_{1.9}\text{O}_4$  were synthesized using  $\text{LiOH}$ ,  $\text{Al}(\text{NO}_3)_3$ , and  $\text{Mn}_3\text{O}_4$  by the melt-impregnation method.  $\text{LiAl}_{0.1}\text{Mn}_{1.9}\text{O}_4$  showed an excellent cycling performance in the 4 V region, but it produced an abrupt capacity loss compared to that of  $\text{LiMn}_2\text{O}_4$  spinel in the 3 V region. From the *ex situ* X-ray diffraction measurements, we observed that the intensities of (311) and (400) peaks for  $\text{LiAl}_{0.1}\text{Mn}_{1.9}\text{O}_4$ , which are typical peaks of cubic phase, gradually increased with cycling and indicated the formation of mixed structure of distinct cubic and tetragonal phases after the third cycle. The increase of cubic phase in the  $\text{LiAl}_{0.1}\text{Mn}_{1.9}\text{O}_4$  structure prevented complete structural change from cubic ( $\text{Li}_{1.0}\text{Mn}_2\text{O}_4$ ) to tetragonal ( $\text{Li}_2\text{Mn}_2\text{O}_4$ ) in the 3 V region. This phenomenon might be one of the major origins of a severe capacity loss for  $\text{LiAl}_{0.1}\text{Mn}_{1.9}\text{O}_4$  material in the 3 V region. © 2001 The Electrochemical Society. [DOI: 10.1149/1.1374038] All rights reserved.

Manuscript submitted August 29, 2000; revised manuscript received February 1, 2001. Available electronically April 30, 2001.

$\text{LiMn}_2\text{O}_4$  spinel is considered one of the most promising cathode materials for lithium secondary batteries because of low cost, abundance, and nontoxicity. However, wide usage of this material in the battery industry is still prevented due to its poor cycling performance compared to that of  $\text{LiCoO}_2$  material.<sup>1,2</sup>

The origin of capacity fade of  $\text{LiMn}_2\text{O}_4$  compound between 4.3 and 3.5 V has been suggested to be (i) the dissolution of  $\text{LiMn}_2\text{O}_4$  electrode material in electrolytes by the disproportionation reaction ( $2\text{Mn}^{3+} \rightarrow \text{Mn}^{4+} + \text{Mn}^{2+}$ ),<sup>3</sup> (ii) the formation of unstable two-phase regions at high voltage regions,<sup>4</sup> (iii) the decomposition of electrolyte at high potentials,<sup>5</sup> and (iv) Jahn-Teller distortion formed at the end of discharge state ( $>3.0$  V).<sup>6</sup>

In the 3 V region (3.5–2.0 V), lithium ions are reversibly inserted/extracted into the 16c octahedral site of spinel ( $\text{Li}_x\text{Mn}_2\text{O}_4$ ) structures ( $1 < x \leq 2$ ). The plateau occurring in this region shows the coexistence of cubic and tetragonal phases in the X-ray diffraction (XRD) study. These tetragonal phases are supposedly formed by Jahn-Teller distortion, which induces the increase of *c/a* ratio of the spinel unit cell about 16%. This brings about a severe capacity fading in the 3 V region.<sup>7,8</sup>

Several research groups<sup>9,10</sup> have attempted to overcome this problem by synthesizing lithium rich spinels or aluminum ion-doped spinels. The spinel structure becomes more tolerant to repeated charge/discharge processes by doping aluminum for manganese. The Al–O bond enhances the strength of  $\text{LiMn}_2\text{O}_4$  structure because the Al–O bond (512 kJ/mol) is stronger than the Mn–O bond (402 kJ/mol) in the octahedron, improving the cyclability of  $\text{LiMn}_2\text{O}_4$  spinel in the 4 V region.

Recent research has focused on the development of high energy density cathode materials operating in the wide voltage region (2.0–4.6 V).<sup>11</sup> However, the use of nonspinel oxides in the (3 + 4) V region encounters many difficulties, such as the transformation of their structures to more stable spinel phase and the capacity loss in the low or high voltage regions.

We have already reported the synthesis of  $\text{LiAl}_x\text{Mn}_{2-x}\text{O}_4$  material, which produces a high discharge capacity as well as an excellent cyclability in both the 3 and 4 V regions. We have also introduced a novel concept on the structural change of  $\text{LiAl}_x\text{Mn}_{2-x}\text{O}_4$  in the 3 V region.<sup>12,13</sup> In this paper, we report that  $\text{LiAl}_x\text{Mn}_{2-x}\text{O}_4$  showed an excellent capacity retention in the 4 V region, but capacity fading of  $\text{LiAl}_x\text{Mn}_{2-x}\text{O}_4$  was more severe than that of  $\text{LiMn}_2\text{O}_4$  spinel in the 3 V region. This is an interesting result because  $\text{LiAl}_x\text{Mn}_{2-x}\text{O}_4$  showed conflicting cycle behavior according to the

operating voltage range. It is impossible to explain this phenomenon within the Jahn-Teller distortion that is believed to be the main reason for capacity loss in the 3 V region.

In this paper, we report this peculiar cycle behavior of  $\text{LiAl}_x\text{Mn}_{2-x}\text{O}_4$  and suggest another reason for inducing severe capacity loss of  $\text{LiAl}_x\text{Mn}_{2-x}\text{O}_4$  material in the 3 V region.

### Experimental

$\text{LiMn}_2\text{O}_4$  and  $\text{LiAl}_{0.1}\text{Mn}_{1.9}\text{O}_4$  materials were synthesized using  $\text{LiOH}$ ,  $\text{Al}(\text{NO}_3)_3$  (Katayama Chemical, Japan), and  $\text{Mn}_3\text{O}_4$  (Tosho, Japan) by melt-impregnation method. The mixture of  $\text{LiOH}$ ,  $\text{Al}(\text{NO}_3)_3$ , and  $\text{Mn}_3\text{O}_4$  was precalcined at 470 and 530°C for 5 h in  $\text{O}_2$ , respectively, and then post-calcined at 800°C for 24 h in air. The contents of Li, Al, and Mn in the resulting materials were analyzed with inductively coupled plasma (ICP) by dissolving the powder in dilute nitric acid. The powder XRD (Rint 1000, Rigaku) using  $\text{Cu K}\alpha$  radiation was employed to identify the crystalline phase of the synthesized material and *ex situ* electrode cell. To investigate the structural change of the positive electrode after the cycles, each tested cell was left in a dry room for 2 days to reach equilibrium after the cycling and the electrode was washed with dimethyl carbonate (DMC) solution to remove  $\text{LiPF}_6$  salt. The electrochemical characterizations were performed using a CR2032 coin-type cell and a screw cell. The cathode was fabricated with 20 mg (or 25 mg for the screw cell) of active material and 12 mg (or 18 mg for the screw cell) of conductive binder [8 mg of Teflonized acetylene black (TAB) and 4 mg of graphite]. This was pressed onto 25 mm<sup>2</sup> stainless steel mesh used as the current collector under a pressure of 300 kg/cm<sup>2</sup> and dried at 200°C for 5 h in an oven. The test cell was made of a cathode and a lithium metal anode (Cyprus Foote Mineral Co.) separated by a porous polypropylene film (Celgard 3401). The electrolyte used was a mixture of 1 M  $\text{LiPF}_6$ -ethylene carbonate (EC)/DMC (1:2 by volume). The charge and discharge current density was 0.4 mA/cm<sup>2</sup> with the cutoff voltages of 2.2 to 3.6 V for 3 V test (or 3.0–4.3 V for 4 V test).

### Results and Discussion

The chemical analysis showed that the powder compositions were  $\text{LiMn}_2\text{O}_4$  and  $\text{LiAl}_{0.1}\text{Mn}_{1.9}\text{O}_4$ . The lattice constants of a cubic unit cell calculated by Rietveld refinement using the XRD data were 8.240 and 8.227 Å for  $\text{LiMn}_2\text{O}_4$  and  $\text{LiAl}_{0.1}\text{Mn}_{1.9}\text{O}_4$ , respectively.

Figure 1 shows the XRD patterns of  $\text{LiMn}_2\text{O}_4$  and  $\text{LiAl}_{0.1}\text{Mn}_{1.9}\text{O}_4$ . All the peaks in the XRD patterns were an indexed single cubic phase with a space group ( $Fd\bar{3}m$ ) and showed that both the prepared materials have an identical crystalline structure. A very small [220] diffraction line at  $2\theta = 30.4^\circ$ , generated by lithium ions remaining at the tetrahedral (8a) sites in the spinel structure, is observable. The position and full width at half-

\* Electrochemical Society Active Member.

<sup>z</sup> E-mail: yoshio@ccs.saga-u.ac.jp

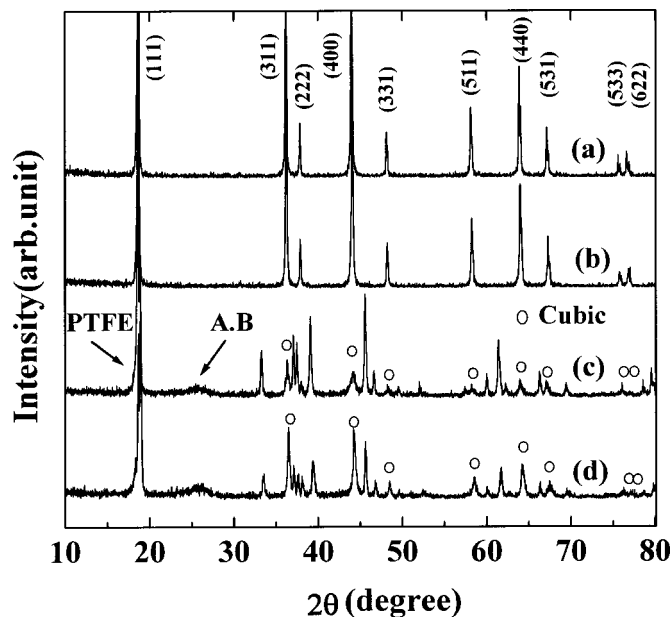


**Figure 1.** XRD patterns for (a)  $\text{LiMn}_2\text{O}_4$  and (b)  $\text{LiAl}_{0.1}\text{Mn}_{1.9}\text{O}_4$  powders. (c)  $\text{LiMn}_2\text{O}_4$  after 50 cycles. (d)  $\text{LiAl}_{0.1}\text{Mn}_{1.9}\text{O}_4$  after 50 cycles.

maximum (fwhm) of the [400] diffraction line have been used to evaluate the degree of crystallization in  $\text{LiMn}_2\text{O}_4$ -based materials. Manev *et al.*<sup>14</sup> reported that the mean lithium content of the spinel can be determined when the (400) peak is located at  $2\theta = 43.95^\circ$  with the fwhm of  $0.1^\circ$ . Our data measured through a silicon reference correction were accurately in agreement with that of the previously reported data.<sup>14</sup> In the XRD patterns after 50 cycles of two materials, these are referred to in Fig. 3.

Figure 2 shows the discharge curves of  $\text{LiMn}_2\text{O}_4$  and  $\text{LiAl}_{0.1}\text{Mn}_{1.9}\text{O}_4$  materials at different voltage regions. Stoichiometric  $\text{LiMn}_2\text{O}_4$  spinel exhibits a typical capacity decline in the 4 V region. This is due to the many reasons described previously.<sup>3-6</sup> In the 3 V region,  $\text{LiMn}_2\text{O}_4$  spinel shows fairly large capacity loss until the fifth cycle, and then gradually decreases discharge capacity until the fiftieth cycle. It has been reported that  $\text{LiMn}_2\text{O}_4$  spinel shows a severe capacity loss as a result of Jahn-Teller distortion when the lithium ion is inserted into the 16c site of  $\text{Li}_x\text{Mn}_2\text{O}_4$  ( $1 < x \leq 2$ ).<sup>7,8</sup>

$\text{LiAl}_{0.1}\text{Mn}_{1.9}\text{O}_4$  material shows an excellent cycle performance in the 4 V region. The capacity retention rate of  $\text{LiAl}_{0.1}\text{Mn}_{1.9}\text{O}_4$  is over 96% after 50 cycles (from 129 to 123 mAh/g), although the initial discharge capacity is lower than that of stoichiometric  $\text{LiMn}_2\text{O}_4$  spinel. This indicates that Al ions are substituted into the octahedral (16d) sites and reduce the amount of  $\text{Mn}^{3+}$  ions in the spinel structure. This results from the increase of average Mn valence and reduces the Jahn-Teller effect. Therefore, Al-doped spinel must show good cycle behavior in the 4 V region with a reduced initial discharge capacity as observed in our previous report.<sup>12,15</sup>

Meanwhile, it is interesting to see the results of the cycle test for  $\text{LiAl}_{0.1}\text{Mn}_{1.9}\text{O}_4$  in the 3 V region. The discharge capacity abruptly declines within the fifth cycle from 124 to 61 mAh/g, but steadily decreases to  $\sim 45$  mAh/g until the fiftieth cycle. This capacity fading is much more severe than that of stoichiometric  $\text{LiMn}_2\text{O}_4$  spinel (from 118 to 100 mAh/g until the fifth cycle) in the same voltage region. The capacity loss percentages of  $\text{LiMn}_2\text{O}_4$  and  $\text{LiAl}_{0.1}\text{Mn}_{1.9}\text{O}_4$  after the fifth cycle were 45 and 76%, respectively. These results lead to the following possible explanation: the capacity fading due to Jahn-Teller distortion in the 3 V region occurs mainly in the early stage of the cycling. Furthermore, the capacity

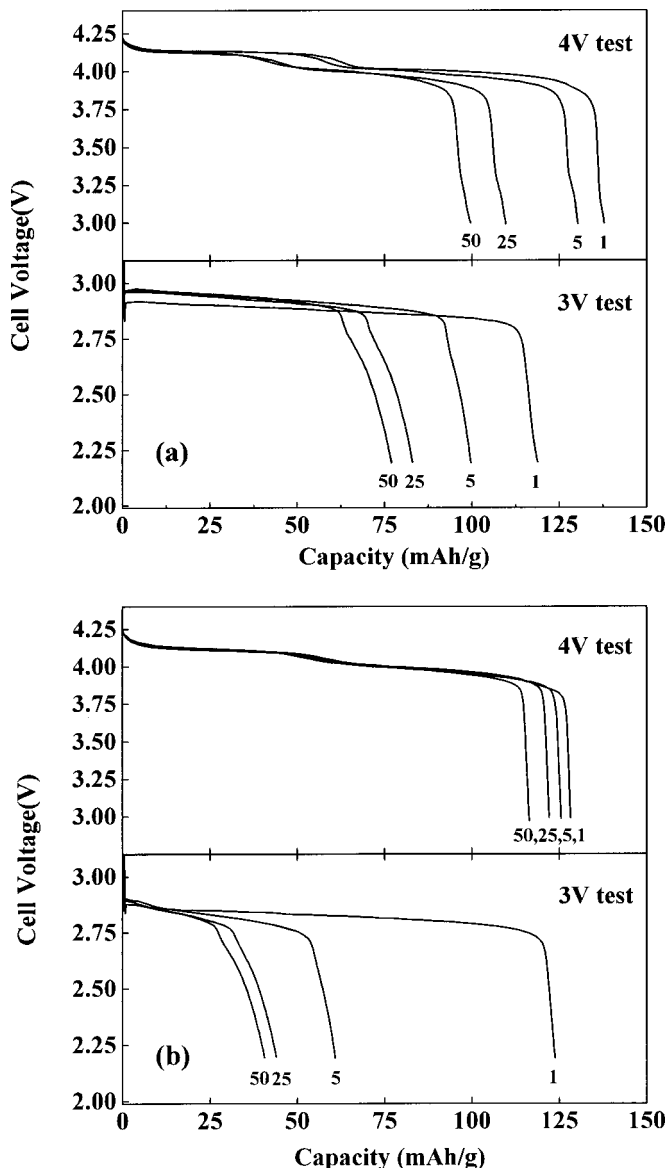


**Figure 2.** Charge/discharge curves of (a)  $\text{LiMn}_2\text{O}_4$  and (b)  $\text{LiAl}_{0.1}\text{Mn}_{1.9}\text{O}_4$  at different voltage regions. Cycling was carried out at a constant charge/discharge current density of  $0.4 \text{ mA/cm}^2$  between 2.2 and 3.6 V for 3 V test (3.0-4.3 V for 4 V test).

loss of Al-doped spinel in the 3 V region may be due to effects other than the Jahn-Teller distortion.

To interpret this particular cycling behavior observed from the  $\text{LiAl}_{0.1}\text{Mn}_{1.9}\text{O}_4$  materials, *ex situ* XRD measurements were taken for  $\text{LiMn}_2\text{O}_4$  and  $\text{LiAl}_{0.1}\text{Mn}_{1.9}\text{O}_4$  electrodes at discharged state after the first to third cycles as shown in Fig. 3. Each set of three cells were disassembled in the argon filled dry box after being tested from 2.2 to 3.6 V.

Figure 3a shows that  $\text{LiMn}_2\text{O}_4$  has a mixed structure consisting of a distinct tetragonal phase and a small amount of cubic phase after the first cycle. The cubic peaks of  $\text{LiMn}_2\text{O}_4$  maintain almost the same intensities to the third cycle, although the (400) diffraction line slightly increases. Furthermore, we also observed the preservation of the similar cubic diffraction line even after 50 cycles, as shown in Fig. 1c.<sup>13</sup>

However, Fig. 3b shows that the intensities of cubic peaks for  $\text{LiAl}_{0.1}\text{Mn}_{1.9}\text{O}_4$  electrode gradually increase with the cycle to be higher than those of tetragonal peaks after three cycles. Addition-

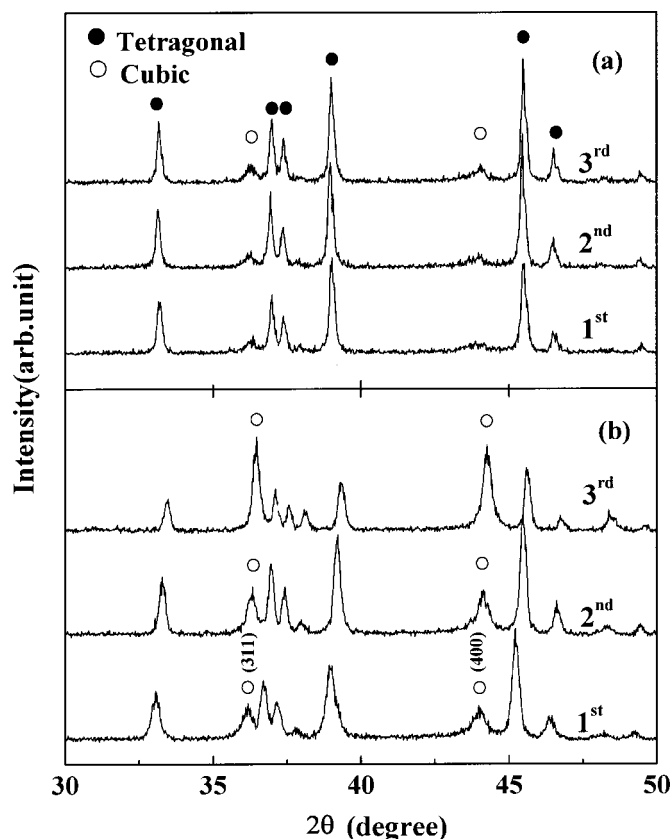


**Figure 3.** *Ex situ* XRD patterns of (a)  $\text{LiMn}_2\text{O}_4$  and (b)  $\text{LiAl}_{0.1}\text{Mn}_{1.9}\text{O}_4$  after the first through third discharges.

ally, all the XRD patterns of  $\text{LiAl}_{0.1}\text{Mn}_{1.9}\text{O}_4$  shift to a higher angle with the cycling.

It is interesting to know there is a great difference in the XRD patterns of  $\text{LiMn}_2\text{O}_4$  and  $\text{LiAl}_{0.1}\text{Mn}_{1.9}\text{O}_4$  materials. This is thought to be because Al-ion plays an important role in the  $\text{LiAl}_{0.1}\text{Mn}_{1.9}\text{O}_4$  material. When lithium ions were inserted into the  $\text{LiAl}_{0.1}\text{Mn}_{1.9}\text{O}_4$  spinel structure at the first discharge in the 3 V region, the material showed almost the same XRD pattern as that of  $\text{LiMn}_2\text{O}_4$  spinel. This means that  $\text{LiAl}_{0.1}\text{Mn}_{1.9}\text{O}_4$  material in the first discharge also can be converted from cubic to tetragonal phase without any disturbance as observed for  $\text{LiMn}_2\text{O}_4$  in the 3 V region. However, the great increase of cubic phase in the XRD patterns measured after the second and third cycles, compared with that of  $\text{LiMn}_2\text{O}_4$ , hinders the structural change from cubic to tetragonal phases. In other words, the intensified cubic phase of  $\text{LiAl}_{0.1}\text{Mn}_{1.9}\text{O}_4$  improves the cyclability of  $\text{LiAl}_{0.1}\text{Mn}_{1.9}\text{O}_4$  in the 4 V region, but prevents complete lithium insertion/extraction into the spinel structure with the cycles in the 3 V region.

Figure 4 shows the results of the constant current and constant voltage (CCCV) test for  $\text{LiMn}_2\text{O}_4$  and  $\text{LiAl}_{0.1}\text{Mn}_{1.9}\text{O}_4$  materials in the 3 V region. This test was conducted to check the degree of lithium insertion/extraction into spinel structure. The charge/discharge time was 600 min and the current density was  $0.4 \text{ mA/cm}^2$  with the cutoff voltage ranging from 2.2 to 3.6 V. The test results strongly support our suggestion about the aluminum effect in the 3 V region. As shown in Fig. 4, two materials show wide differences in the discharge capacity in the (a) region. The different cycle behavior of two materials in the (a) region can be explained as follows. The capacity loss of  $\text{LiMn}_2\text{O}_4$  in this region results from only Jahn-Teller distortion as explained previously. However, the capacity decline of  $\text{LiAl}_{0.1}\text{Mn}_{1.9}\text{O}_4$  in this region is thought to be due to both the Jahn-Teller distortion and the strong

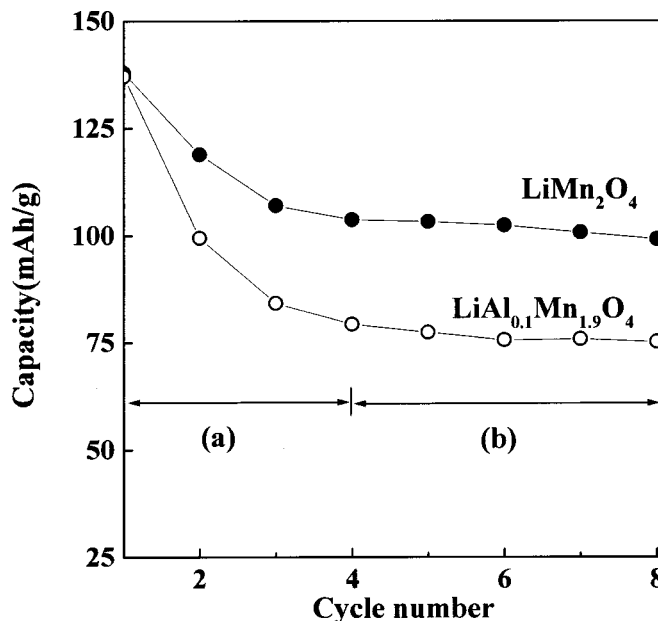


**Figure 4.** CCCV test for  $\text{LiMn}_2\text{O}_4$  and  $\text{LiAl}_{0.1}\text{Mn}_{1.9}\text{O}_4$  materials in the 3 V region.

increase of cubic phase by the effect of aluminum ion. Therefore, this results in irreversible lithium insertion/extraction into spinel structure on cycling and  $\text{LiAl}_{0.1}\text{Mn}_{1.9}\text{O}_4$  material shows a severe capacity fade more than that of  $\text{LiMn}_2\text{O}_4$  in the (a) region.

In addition, the capacity of two materials in the (b) region shows a slight decrease. This also can be explained by the fact that all lithium ions inserted into spinel structure in the first discharge process are unable to attend the second discharge process because of the hindrance of Jahn-Teller distortion or the aluminum effect. After the fourth cycle, where the severe capacity fading mostly ends, only fixed amounts of lithium ions can insert/extract into its spinel structure perfectly. Therefore,  $\text{LiAl}_{0.1}\text{Mn}_{1.9}\text{O}_4$  can maintain a stable cycle performance after the fourth cycle in the CCCV test.

On the basis of these results, we conclude that the capacity fading due to Jahn-Teller distortion occurs mainly in the early stage of the cycling in the 3 V region and the intensified cubic phase peaks on cycling might act as an inhibitor which prevents complete lithium insertion/extraction into the spinel structure in the 3 V region.

### Conclusion

We have synthesized  $\text{LiMn}_2\text{O}_4$  and  $\text{LiAl}_{0.1}\text{Mn}_{1.9}\text{O}_4$  by the melt-impregnation method.  $\text{LiAl}_{0.1}\text{Mn}_{1.9}\text{O}_4$  showed excellent cycle performance in the 4 V region, but an abrupt capacity loss in the 3 V region. The intensities of (311) and (400) peaks of  $\text{LiAl}_{0.1}\text{Mn}_{1.9}\text{O}_4$  gradually increased with cycling and indicated the formation of a mixed structure of distinct cubic and tetragonal phases after the third cycle. The increase in cubic phase of the  $\text{LiAl}_{0.1}\text{Mn}_{1.9}\text{O}_4$  prevented complete structural change from cubic ( $\text{Li}_{1.0}\text{Mn}_2\text{O}_4$ ) to tetragonal ( $\text{Li}_2\text{Mn}_2\text{O}_4$ ) in the 3 V region. This phenomenon could be another major factor, together with Jahn-Teller distortion, in the severe capacity loss of  $\text{LiAl}_{0.1}\text{Mn}_{1.9}\text{O}_4$  material in the 3 V region.

Saga University assisted in meeting the publication costs of this article.

### References

1. J. N. Reimers, E. W. Fuller, E. Rossen, and J. R. Dahn, *J. Electrochem. Soc.*, **140**, 3396 (1993).
2. J. M. Tarascon, W. R. Mckinnon, F. Coowar, T. N. Bowmer, G. Amatucci, and D. Guyomard, *J. Electrochem. Soc.*, **141**, 1421 (1994).
3. D. H. Jang, Y. J. Shin, and S. M. Oh, *J. Electrochem. Soc.*, **143**, 2204 (1996).
4. Y. Xia, Y. Zhou, and M. Yoshio, *J. Electrochem. Soc.*, **144**, 2593 (1997).
5. D. Guyomard and J. M. Tarascon, *J. Electrochem. Soc.*, **139**, 937 (1992).

6. M. M. Thackeray, Y. Shao-Horn, A. J. Kahaian, K. D. Kepler, E. Skinner, J. T. Vaughey, and S. A. Hackney, *Electrochem. Solid-State Lett.*, **1**, 7 (1998).
7. M. M. Thackeray, P. G. David, P. G. Bruce, and J. B. Goodenough, *Mater. Res. Bull.*, **18**, 461 (1983).
8. J. Barker, R. Koksang, and M. Y. Saidi, *Solid State Ionics*, **82**, 143 (1995).
9. F. Le Cras, D. Bloch, M. Anne, and P. Strobel, *Solid State Ionics*, **89**, 203 (1996).
10. D. Song, H. Ikuta, T. Uchida, and M. Wakihara, *Solid State Ionics*, **117**, 151 (1999).
11. J. M. Paulsen, J. R. Mueller-Neuhaus, and J. R. Dahn, *J. Electrochem. Soc.*, **147**, 508 (2000).
12. Y. S. Lee, N. Kumada, and M. Yoshio, *J. Power Sources*, **96**, 376 (2001).
13. Y. S. Lee, H. j. Lee, and M. Yoshio, *Electrochem. Commun.*, **3**, 20 (2001).
14. V. Manev, T. Faulkner, and J. Engel, in *Proceedings of the First Hawaii Battery Conference*, p. 228 (1998).
15. Y. M. Todorov, Y. Hdesima, H. Noguchi, and M. Yoshio, *J. Power Sources*, **77**, 198 (1999).